RevMexAA (Serie de Conferencias), **1**, 229-236 (1995)

BOUNDARY LAYER SOLUTIONS FOR T TAURI AND FU ORIONIS STARS

Robert Popham

Department of Physics, University of Illinois
Loomis Lab, 1110 W. Green St., Urbana, IL 61801, USA

Ramesh Narayan, Scott J. Kenyon, and Lee Hartmann

Harvard-Smithsonian Center for Astrophysics
60 Garden St., Cambridge, MA 02138, USA

RESUMEN

Se presentan soluciones de la estructura de la capa límite que se origina donde el disco de acrecimiento encuentra la superficie estelar de estrellas de la presecuencia principal, para luego comparar estas soluciones con observaciones de estrellas T Tauri y FU Orionis.

ABSTRACT

We present solutions for the structure of the boundary layer that occurs where the accretion disk meets the stellar surface of accreting pre-main-sequence stars. These solutions were calculated using a "slim disk"-type model which treats the disk and boundary layer structure in a somewhat more sophisticated way than the standard geometrically thin disk model. They describe both the flow of the accreting gas and the radiation produced by the accretion. The luminosity of the boundary layer is comparable to that of the disk, making it an important component in the spectra of accreting pre-main-sequence stars.

Solutions calculated for the $\sim 10^{-7}\ M_\odot\ \mathrm{yr}^{-1}$ accretion rates commonly ascribed to T Tauri stars produce boundary layers with effective temperatures $\sim$ 8500 K and emitting areas of a few percent of the area of the stellar surface. These agree well with the temperatures and sizes derived from simple slab models used to fit the blue continuum excess ("veiling") emission observed in T Tauri spectra. The luminosity of the boundary layer in these solutions is comparable to that of the disk or star, while its effective temperature is substantially higher, so that radiation from the boundary layer appears as a distinct component in the spectrum.

Solutions for the much larger, $\sim 10^{-4}\ M_\odot\ \mathrm{yr}^{-1}$ rates attributed to FU Orionis stars produce wide boundary layers with effective temperatures similar to those in the inner disk. As a result, the disk and boundary layer components are difficult to distinguish in the spectrum. Comparison with photometric observations of V1057 Cygni show that a stellar radius of $\sim 6R_\odot$ or larger is required to match the small flux observed in the ultraviolet. Solutions with rotation rates comparable to those observed in T Tauri stars match the photometric observations, and can have negative angular momentum accretion rates, suggesting that FU Orionis outbursts could play a role in limiting the spin-up of T Tauri stars.

Key words: **ACCRETION, ACCRETION DISKS— STARS: PRE-MAIN-SEQUENCE**

1. INTRODUCTION

The boundary layer is the transition between the accretion disk and the accreting star. Within this region, the rotation rate of the accreting material drops from near-Keplerian in the disk to the stellar rotation rate in the star. The boundary layer is very important to studies of accreting systems because it contributes up to half of the total luminosity produced by accretion.

The total accretion luminosity is

$$L_{acc} = \frac{GM_*\dot{M}}{R_*}.$$

The disk luminosity derived from integrating the standard thin disk relation for the flux from the disk surface is

$$L_{disk} = \int_{R_*}^{\infty} \frac{3GM_*\dot{M}}{8\pi R_*^3}\left(1-\left(\frac{R_*}{R}\right)^{1/2}\right)\cdot 2\pi R\cdot 2\cdot dR = \frac{GM_*\dot{M}}{2R_*} = \frac{1}{2}L_{acc}.$$

So half of the gravitational potential energy is radiated in the disk; the remaining half is in the form of rotational kinetic energy:

$$\frac{1}{2}\dot{M}v_K^2(R_*) = \frac{GM_*\dot{M}}{2R_*} = \frac{1}{2}L_{acc}$$

A large fraction of this energy can be dissipated and radiated from the boundary layer region.

In order to better understand the boundary layer and its effect on the emitted spectrum, we want to know how much of the rotational energy is radiated, and in what part of the spectrum this energy is radiated. To answer these questions, we need to know the size of the shearing region where the energy is dissipated, and the size and optical depth of the emitting region where the energy is radiated. Therefore, we need a model which describes the flow of the accreted material and the accretion energy.

2. BOUNDARY LAYER MODEL

The boundary layer represents the transition from the disk to the star, two regions which have quite different physical characteristics. The material in the disk is supported against gravity by rotation, whereas in the star the dominant source of radial support is the pressure gradient. Also, in the disk, radiation carries energy vertically, from the midplane to the surface, while in the star, the radiative transport is radial.

The standard thin disk equations assume that the terms which become important in the star, such as pressure support and radial radiation, can be ignored in the disk; clearly they cannot be ignored in the boundary layer. We need improved disk equations which include these terms. Equations of this type were developed for work on accretion disks around black holes by Paczyński and collaborators (Paczyński & Bisnovatyi-Kogan 1981, Muchotrzeb & Paczyński 1982, Abramowicz et al. 1988), and are known as "slim disk" equations.

Here, we list the thin disk and slim disk versions of the radial momentum, angular momentum, and energy equations:

	Thin Disk	Slim Disk
Radial momentum:	$\Omega = \Omega_K$	$(\Omega^2 - \Omega_K^2)R = \frac{1}{\rho}\frac{dP}{dR} + v_R\frac{dv_R}{dR}$
Angular momentum:	$\dot{J} = \dot{M}\Omega_K(R_*)R_*^2$	$\dot{J} = j\dot{M}\Omega_K(R_*)R_*^2$
	$\nu\Sigma = \frac{\dot{M}}{6\pi}\left[1-\left(\frac{R_*}{R}\right)^{1/2}\right]$	$\dot{J} = \dot{M}R^2\left(\Omega - \frac{\nu}{v_R}\frac{d\Omega}{dR}\right)$
Energy:	$F_V = \frac{3GM_*\dot{M}}{8\pi R^3}\left[1-\left(\frac{R_*}{R}\right)^{1/2}\right]$	$F_V = \nu\Sigma\left(R\frac{d\Omega}{dR}\right)^2 - v_R\Sigma T\frac{dS}{dR} - \frac{1}{4\pi R}\frac{d}{dR}(4\pi RHF_R)$

In the thin disk, Ω is assumed to be Keplerian at all radii, so that rotation provides full support against gravity. In the slim disk, radial pressure gradients and the radial acceleration of the disk material are included in the radial momentum balance. Both the thin and slim disk formulations use the same angular momentum equation, which gives the rate of angular momentum transfer as the sum of the angular momentum carried by the accreting material and the angular momentum transferred by viscous torque. In the thin disk formulation, the assumption of Keplerian rotation allows this equation to be simplified considerably, and the total angular momentum transfer rate is assumed to be just the product of the mass accretion rate and the Keplerian specific angular momentum at the stellar surface. The slim disk approach avoids these assumptions. Finally, the thin disk energy equation assumes that all the energy dissipated by viscosity at a given radius is radiated from the disk surface at that same radius. The slim disk version also includes radial transfer of energy by radiation and by the infalling gas.

In our boundary layer model, we use the slim disk equations listed above. To these we add equations for simple two-stream radiative transport in the radial and vertical directions, an alpha-type viscosity prescription, an equation of state which includes gas and radiation pressure, and a tabulated opacity. More details about the model are given in Popham et al. (1993).

3. T TAURI BOUNDARY LAYERS

Spectra of T Tauri stars show "veiling" of stellar photospheric absorption lines by blue excess continuum emission. Basri & Bertout (1989) and Hartigan et al. (1991) fitted the spectrum of the continuum emission in several T Tauri stars using a single-temperature slab model to find the characteristic temperature T_{eff} and area A of the emitting region, and found

$$T_{eff} \simeq 7000 - 10,000 \text{ K},$$

$$A \simeq 0.01 - 0.1 A_*,$$

where A_* is the area of the stellar surface.

We can compare this to the boundary layer solution shown in Figure 1, which was calculated using the "slim disk" equations described above, and standard estimates for the T Tauri star mass, radius, and mass accretion rate: $M_* = 1\ M_\odot, R_* = 1.5 \times 10^{11}$ cm $= 2.15\ R_\odot, \dot{M} = 10^{-7}\ M_\odot$ yr^{-1}. The angular velocity Ω drops rapidly in a narrow dynamical boundary layer, but the energy dissipated is radiated from a larger thermal boundary layer. The boundary layer region in the solution has a peak $T_{eff} \simeq 8500$ K, and the boundary layer luminosity is emitted from an area which is a few percent of the area of the stellar surface. Note that the dip in the effective temperature in the outer portion of the thermal boundary layer is due to opacity effects. The disk remains thin even in the boundary layer region; the vertical pressure scale height is only $\sim 5\%$ of the radius. Figure 2 shows a blackbody spectrum for this solution, which shows two peaks corresponding to the boundary layer and disk. Note that we have not included any stellar flux in the spectrum.

4. FU ORIONIS BOUNDARY LAYERS

Spectra of FU Ori and V1057 Cyg were fitted with disk models (with no boundary layer) by Kenyon, Hartmann, & Hewett (1988); they found $T_{max} \simeq 6500 - 7000$K. Note that for a standard thin disk,

$$T_{eff} = \left(\frac{3GM_*\dot{M}}{8\pi\sigma R_*^3}\right)^{1/4} \left[1 - \left(\frac{R_*}{R}\right)^{1/2}\right]^{1/4},$$

so that T_{max} occurs at $R = 49/36 R_*$, and

$$T_{max} = 0.287 \left(\frac{GM_*\dot{M}}{\sigma R_*^3}\right)^{1/4}$$

Fitting the infrared part of the spectrum produced by the outer disk requires $M_*\dot{M} \simeq 5 \times 10^{-5}\ M_\odot$ yr^{-1}, which produces $T_{max} \simeq 6500$K for $R_* = 3 \times 10^{11}$ cm $= 4.3 R_\odot$. This is already much larger than T Tauri star radii, and no boundary layer has been included. Models which include the boundary layer luminosity will heat

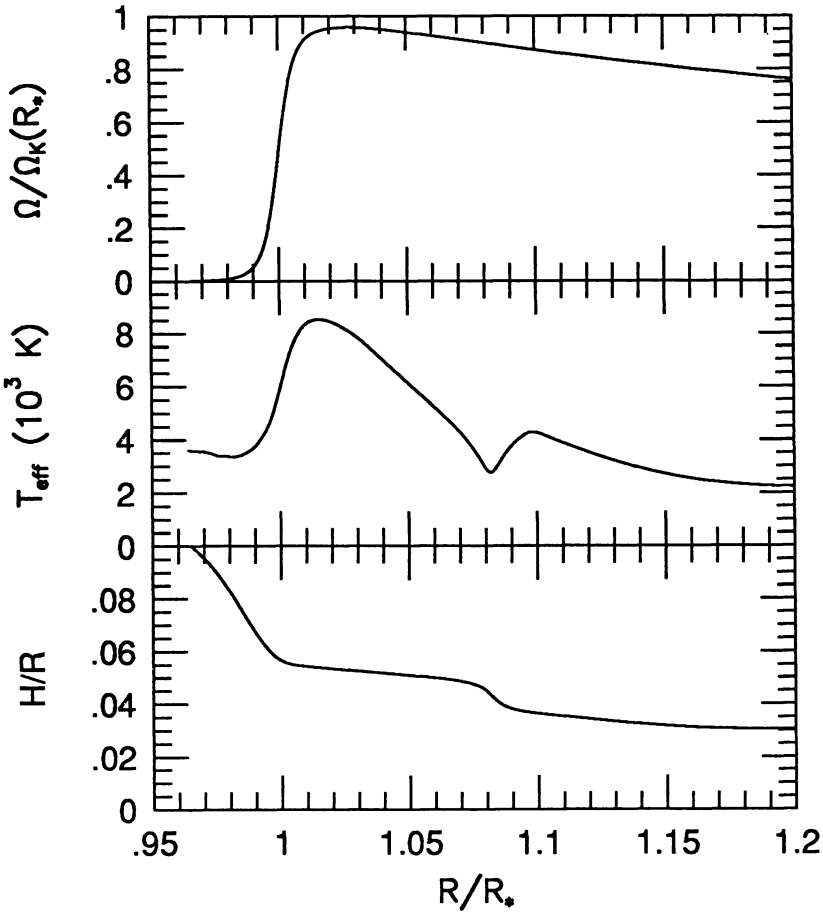

Fig. 1.— A boundary layer solution for T Tauri star parameters: $M_* = 1M_\odot$, $R_* = 1.5 \times 10^{11}$ cm $= 2.15R_\odot$, and $\dot{M} = 10^{-7}\ M_\odot\ \mathrm{yr}^{-1}$. The three panels show the angular velocity Ω, the effective temperature T_{eff} of the disk surface, and the disk thickness H/R.

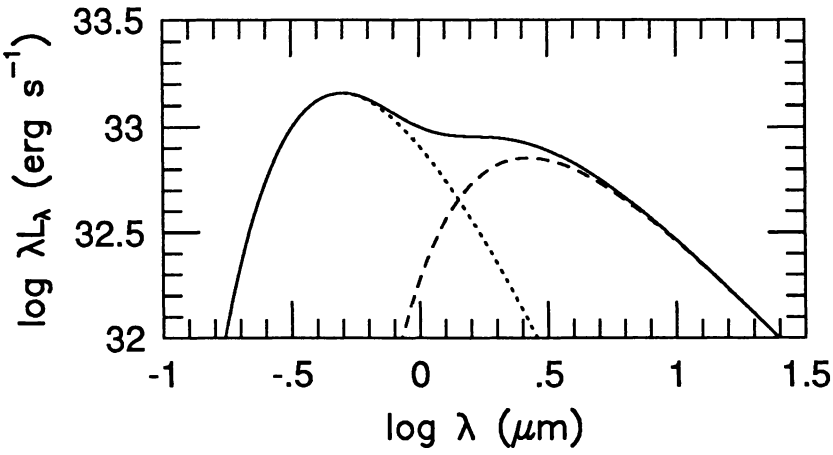

Fig. 2.— The blackbody spectrum of the disk and boundary layer solution shown in Figure 1; the boundary layer component is denoted by a dotted line and the disk component by a dashed line.

the inner disk to even higher temperatures than those predicted by the standard thin disk model; thus even larger stellar radii will be required.

Here we have tried to match photometric data for V1057 Cygni with our solutions which include the boundary layer. Figure 3 shows 2 solutions; one has $\dot{M} = 10^{-4}\ M_\odot\ \mathrm{yr}^{-1}$ and $R_* = 4 \times 10^{11}\ \mathrm{cm} = 5.75 R_\odot$. In the other, both $\dot{M}$ and R_* are twice as large, so that the accretion luminosity remains the same. Both solutions have $M_* = 0.5 M_\odot$, $j \sim 1$, and $\alpha = 0.01$. The boundary layer becomes quite wide in these solutions; the dynamical boundary layer width is comparable to the stellar radius. The angular velocity Ω remains noticeably sub-Keplerian even in the disk. Since the boundary layer is wide, it does not produce the pronounced peak in the effective temperature seen in the T Tauri solution. The disk is also fairly thick in these solutions, with $H/R \sim 0.3 - 0.4$.

Figure 4 shows the blackbody spectra produced by these solutions, compared with V1057 Cygni data. The solution with $\dot{M} = 10^{-4}\ M_\odot\ \mathrm{yr}^{-1}$ and $R_* = 4 \times 10^{11}$ cm fits reasonably well, but the solution with $\dot{M} = 2 \times 10^{-4}\ M_\odot\ \mathrm{yr}^{-1}$ and $R_* = 8 \times 10^{11}$ cm fits the near-infrared portion of the spectrum better. The extinction correction applied to the data ($A_V = 3.5$ mag) is somewhat uncertain, and since the extinction increases at shorter wavelengths, the U-band data point has the largest uncertainty. Note that the symbols used for the data points in Figure 4 are all of the same size, and are not intended to represent the uncertainties in the data. Also, the data point at $\lambda = 10\ \mu$m, and other data points at longer wavelengths not shown in Figure 4, are believed to represent dust emission rather than radiation from the disk, so we do not attempt to match them with our model. Essentially, we have tried to find solutions which produce spectra which match the data points at $\lambda < 10\ \mu$m reasonably well, allowing more room for error in the U-band point.

5. SMALL AND NEGATIVE $\dot{J}$ SOLUTIONS

In standard boundary layer solutions, Ω reaches a maximum at a radius R_{max}, and since the viscous torque is zero at that point, the angular momentum accretion rate $\dot{J}$ is constrained to be

$$\dot{J} = \dot{M} \Omega_{max} R_{max}^2.$$

If the radial extent of the boundary layer is small compared to R_*, then $R_{max} \sim R_*$ and $\Omega_{max} \sim \Omega_K(R_*)$, so that

$$\dot{J} = \dot{M} \Omega_K(R_*) R_*^2, \quad \text{or} \quad j \sim 1,$$

where j is defined as $\dot{J}$ in units of $\dot{M}\Omega_K(R_*)R_*^2$.

A second type of boundary layer solutions has no maximum in Ω; $d\Omega/dR$ is negative everywhere. These solutions can have a wide range of values for j, including $j \leq 0$, so that the star can accrete mass while losing angular momentum. These solutions require the star to be rotating. For a thin disk, $\Omega \simeq \Omega_K$ throughout the disk, so that for there to be no maximum in Ω, the stellar rotation rate Ω_* must be close to the maximum rotation $\Omega_K(R_*)$. FU Orionis disks are moderately thick ($H/R \sim 0.3 - 0.4$), and have substantial pressure support, so that Ω is somewhat sub-Keplerian. Thus we can have solutions with small or negative j even when $\Omega_* < \Omega_K(R_*)$.

For $M_* = 0.5 M_\odot$, $R_* = 4 \times 10^{11}$ cm, we have $\Omega_K(R_*) = 3.2 \times 10^{-5}\ \mathrm{s}^{-1}$. In Figure 5, we show 2 solutions for $\Omega_* = 0.25\Omega_K(R_*)$, which have $j = 0$ and $j = -1$, and one solution for $\Omega_* = 0.5\Omega_K(R_*)$, $j = 0$. The three solutions all have $\dot{M} \sim 10^{-4}\ M_\odot\ \mathrm{yr}^{-1}$, $M_* = 0.5 M_\odot$, $R_* = 4 \times 10^{11}$ cm, and $\alpha = 0.1$. The angular velocity decreases outward throughout the flow in these solutions; there is no real boundary layer. As in the earlier solutions, there is no pronounced peak in T_{eff}, and the disk is moderately thick and sub-Keplerian. Figure 6 shows the blackbody spectra for these solutions, which all fit the data reasonably well.

6. FU ORIONIS OUTBURSTS AND SPIN-UP OF T TAURI STARS

T Tauri stars are observed to be rotating slowly; many of them have rotation rates which are $\sim 10\%$ of their maximum values. This is surprising since disk accretion should spin the accreting star up fairly rapidly, and it has been taken as evidence that T Tauri star accretion may be controlled by strong stellar magnetic fields.

The FU Orionis solutions presented above with $j \leq 0$ have rotation rates similar to those observed in T Tauri stars: $P_{rot} \sim 4.5 - 9$ days. This suggests a scenario in which FU Orionis outbursts could control the spin-up of T Tauri stars:

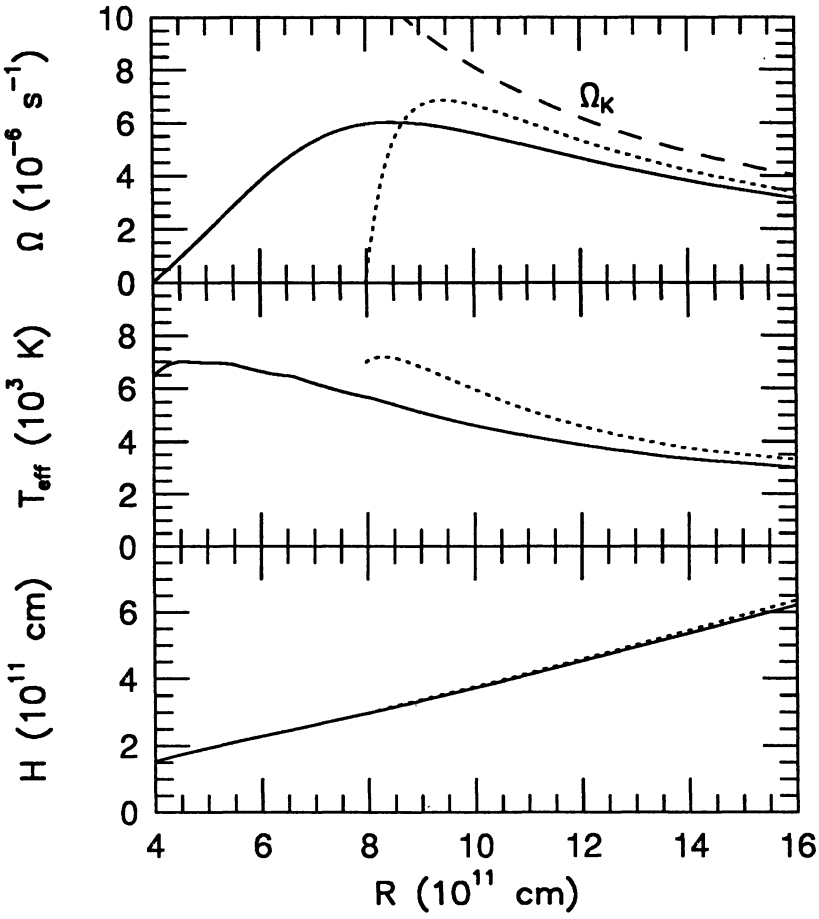

Fig. 3.— Boundary layer solutions for FU Orionis star parameters: one solution has $R_* = 4 \times 10^{11}$ cm, and $\dot{M} = 10^{-4}\ M_\odot\ \mathrm{yr}^{-1}$ (solid line), and the other has $R_* = 8 \times 10^{11}$ cm, and $\dot{M} = 2 \times 10^{-4}\ M_\odot\ \mathrm{yr}^{-1}$ (dashed line). Both solutions have $M_* = 0.5 M_\odot$, $j \sim 1$ and $\alpha = 0.01$.

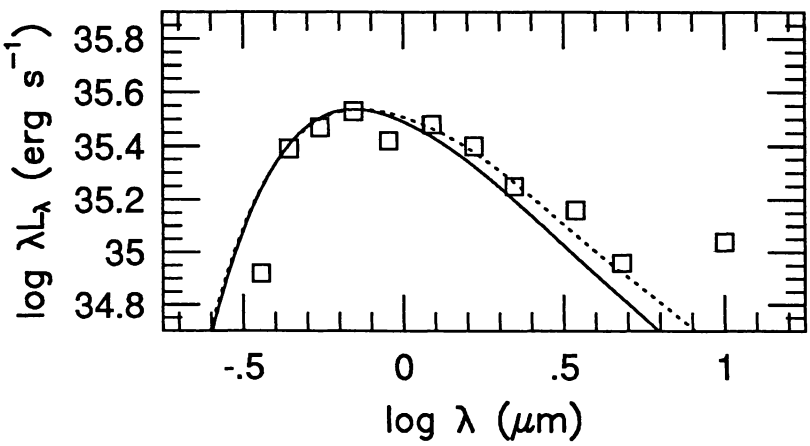

Fig. 4.— The blackbody spectra of the disk and boundary layer solutions shown in Figure 3 and photometric data for V1057 Cygni (square boxes).

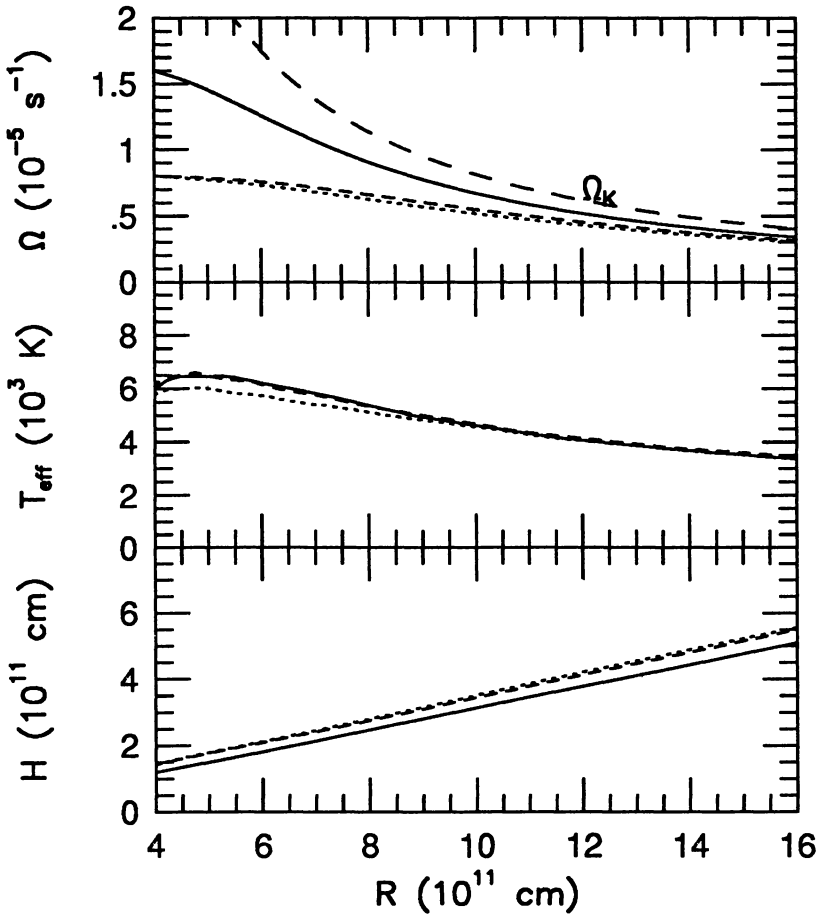

Fig. 5.— Small and negative $\dot{J}$ boundary layer solutions for FU Orionis star parameters: the three solutions all have $R_* = 4 \times 10^{11}$ cm, $M_* = 0.5 M_\odot$, and $\alpha = 0.1$; one has $\Omega_* = 1.6 \times 10^{-5}$ s, $j = 0$, and $\dot{M} = 10^{-4.15}\ M_\odot\ \mathrm{yr}^{-1}$ (solid line), another has $\Omega_* = 8 \times 10^{-6}$ s, $j \doteq -1$, and $\dot{M} = 10^{-4}\ M_\odot\ \mathrm{yr}^{-1}$ (dashed line), and the third has $\Omega_* = 8 \times 10^{-6}$ s, $j = 0$, and $\dot{M} = 10^{-4.2}\ M_\odot\ \mathrm{yr}^{-1}$ (dotted line).

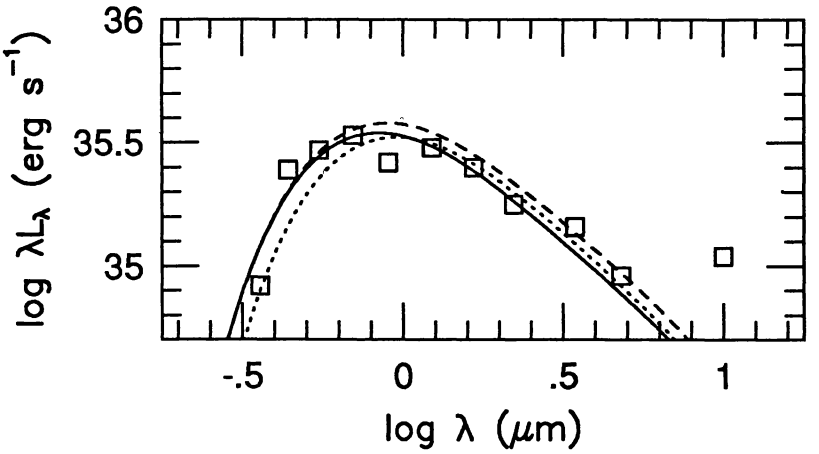

Fig. 6.— The blackbody spectra of the disk and boundary layer solutions shown in Figure 5 and photometric data for V1057 Cygni (square boxes).

In the T Tauri phase, the star spins at $\sim 10\%$ of the maximum rotation ($\Omega_* \sim 0.1\Omega_K(R_*)$). The disk is thin and Ω drops in a narrow boundary layer from $\sim \Omega_K$ to Ω_*. Thus $j \simeq 1$ and the star spins up.

During the FU Orionis outbursts, the stellar radius is substantially larger than in the T Tauri phase. Therefore Ω_* is a larger fraction of $\Omega_K(R_*)$. Also, the disk is much thicker, and so $\Omega < \Omega_K$. Thus the second type of boundary layer with $j < 0$ may be produced, so that the disk removes large amounts of angular momentum from the star.

Since the mass accretion rate is much larger in the FU Orionis outbursts, most of the mass accreted by a star may be added during outbursts rather than during the T Tauri phases. Since $\dot{J} \propto \dot{M}$, the outbursts should also control the angular momentum accretion.

7. CONCLUSIONS

- Boundary layer solutions for T Tauri stars agree with the inferred properties of the emitting region which produces the observed blue excess continuum ("veiling") emission
- Boundary layer solutions for FU Orionis stars require large stellar radii to produce the maximum temperatures of 6500–7000 K required to match observed spectra.
- Boundary layer solutions with small or negative angular momentum accretion rates could be obtained in FU Orionis stars, and could serve to limit the spin-up of T Tauri stars to a small fraction of their maximum rotation rates.

REFERENCES

Abramowicz, M. A., Czerny, B., Lasota, J. P., & Szuszkiewicz, E. 1988, ApJ, 332, 646
Basri, G., & Bertout, C. 1989, ApJ, 341, 340
Hartigan, P., Kenyon, S. J., Hartmann, L., Strom, S. E., Edwards, S., Welty, A. D., & Stauffer, J. 1991, ApJ, 382, 617
Kenyon, S. J., Hartmann, L., & Hewett, R. 1988, ApJ, 325, 231
Muchotrzeb, B., & Paczyński, B. 1982, Acta, 32, 1
Paczyński, B., & Bisnovatyi-Kogan, G. 1981, Acta, 31, 283
Popham, R., Narayan, R., Hartmann, L., & Kenyon, S. 1993, ApJ, 415, L127